Brittle structures at the Stavsjö quarry, Falkenberg

Susanne Grigull & Jenny Andersson

February 2019

SGU-rapport 2019:05

SGU
Sveriges geologiska undersökning
Geological Survey of Sweden

Cover photo: Fractured quartz monzodiorite in the east-facing wall of the Stavsjö quarry
Photographer: Susanne Grigull

Authors: Susanne Grigull & Jenny Andersson
Reviewed by: Philip Curtis
Head of department: Mugdim Islamović
Project name: Bedrock mapping Falkenberg
Project id: 80023

Layout: Johan Sporrong, SGU

Geological Survey of Sweden
Box 670, 751 28 Uppsala
phone: 018-17 90 00
fax: 018-17 92 10
email: sgu@sgu.se
www.sgu.se

Table of Contents

ABSTRACT

In order to obtain information on the brittle deformation history of ductilely deformed gneisses of the Varberg granulite gneiss domain, fracture mapping was performed in a pilot study along three short horizontal profiles at the Stavsjö quarry near Falkenberg. Two dominant fracture sets, striking west-northwest–east-southeast and north-northeast–south-southwest were identified. Dip angles for both sets peak at around 70°–80°. Later reactivation of some fractures shows that the stress field changed after formation of the first, north-northeast–south-southwest striking, fracture set. Overall, the orientations of the fractures measured at Stavsjö quarry match the orientations of regional geophysical lineaments, indicating that these also represent brittle structures.

The north-northeast–south-southwest striking fractures seen in the quarry match well with north-northeast–south-southwest striking fractures and faults in the surrounding gneiss complex as well as on a regional scale in the Eastern Segment. These have been coupled with the development of the Vättern graben fault system and intrusion of dolerite dykes across the south-western Fennoscandia in the Early Neoproterozoic.

The west-northwest–east-southeast striking set is likely linked to a conspicuous west-northwest–east-southeast trending magnetic lineament fringing the Stavsjö quarry that in turn aligns with the major west-northwest–east-southeast trending Sorgenfrei-Tornquist Zone fault system.

In summary, the fracture orientation data collected in the Stavsjö quarry match the orientation of well known regional scale geological and geophysical lineaments in this part of the Fennoscandian continent. This suggests that the brittle structural pattern is scale-independent. It also indicates that limited schematic fracture mapping supports the concept of picking up a large scale picture of the regional scale paleostress field history.

SAMMANFATTNING

Kartläggning av spröda strukturer har utförts längs tre horisontella ca 15 m långa, profiler i en aktiv bergtäkt vid E6:an utanför Falkenberg (Stavsjö bergtäkt). Projektet genomfördes som en pilotstudie för att utveckla metodik vid SGU för kartläggning av spröda strukturer i bergtäkter.

Två dominerande sprickgrupper identifierades: en västnordväst–ostsydostlig, och en nordnordost–sydsydvästlig; båda brant stående (övervägande 70–80°). Reaktivering av en del sprickor indikerar en förändring av stressfältet efter bildningen av den nordnordostliga–sydsydvästliga sprickgenerationen, vilken därför bedöms vara äldst.

Den generella orienteringen av sprickgrupperna i Stavsjötäkten överensstämmer med orienteringen på regionala geofysiskt indikerade lineament. Detta talar för att även dessa representerar spröda deformationsstrukturer.

Den nordnordostliga–sydsydvästliga sprickgruppen överensstämmer väl med nordnordost–sydsydvästliga spröda strukturer (sprickor, sprickzoner och förkastningar) som kartlagts både i närmast omgivande berggrund och i regional skala i Östra Segmentet. Dessa kopplas till förkastningssystemet i Vätternsänkan och den extensionrelaterade diabassvärm som intruderar södra Fennoskandia i tidig Neoproterosoisk tid (Tonian).

Den västnordväst–ostsydostligt orienterade sprickgruppen kopplas till framträdande västnordväst– ostsydostliga magnetiska lineament som löper i anslutning till täkten. Dessa lineament ansluter i sin tur till det storskaliga västnordväst–ostsydostliga förkastningssystemet i Sorgenfrei-Tornquistzonen.

Sprickdata som insamlats i de tre profilerna från Stavsjötäkten överensstämmer väl med storskaliga spröda deformationsstrukturer och geofysiska lineament som tidigare kartlagts i denna del av den

Fennoskandiska kontinenten. Detta indikerar att det spröda deformationsmönstret inte är skalberoende och att begränsad schematisk kartläggning av spröda strukturer kan användas för karaktärisering av det generella regionala paleostressfältet.

INTRODUCTION

Motivation

In the past, the SGU bedrock mapping programme has paid little attention to brittle structures and there are at present no standardised routines for how to record them during field work. Quantifying, analysing, and understanding brittle structures are, however, essential if we are to understand subjects such as paleostress, rock stability, rock quality, and groundwater pathways.

This study was designed as a pilot study with the aim to test the outcome of a one day effort of mapping brittle structures in a restricted area of a quarry. The Stavsjö quarry (Fig. 1, 6312927/0347479) near Falkenberg, was chosen for several reasons: it is located within an area that was the focus of ongoing bedrock mapping and investigations of the suitability of the bedrock for aggregate production (road and concrete; cf. Andersson et al., in press). The rocks in the quarry are relatively homogeneous, implying that fracture formation does not depend on rock type; a quarry gives insight into the extent of brittle structures in three dimensions. In addition, a MSc study was carried out on these rocks (Lundgren 2012), providing information on their mineralogical and chemical composition as well as other rock mechanical parameters.

Geological setting

The Stavsjö quarry is located in the internal section of the Eastern Segment of the Sveconorwegian orogen (Fig. 1A), which is dominated by granitic to granodioritic and quartz monzodioritic migmatitic orthogneisses, representing the reworked equivalents to 1.74–1.66 Ga igneous rocks of the Transscandinavian Igneous Belt (Petersson et al., 2015; Möller et al., 2015). The quarry is dominated by poly-metamorphic high-grade grey to reddish grey migmatitic orthogneiss of quartz monzonitic to quartz monzodioritic composition. Migmatisation is heterogeneous and veining is generally discrete to moderate. Remnants of a relict igneous, coarse to medium grained, inequigranular fabric or a relict augen texture defined by pinkish K-feldspar-rich aggregates are observed in places.

The rocks in the Stavsjö pit are more hydrated and more statically recrystallized than surrounding rocks of the Varberg granulite gneiss domain that generally preserve a dry high-temperature mineralogy (Lundgren 2012). In contrast to the surrounding gneisses, the Stavsjö gneiss has been pervasively recrystallized under hydrous amphibolite facies conditions, and has a mineral assemblage with tartan twinned microcline, plagioclase, and quartz, deep green to olive green hornblende, brown biotite and oxides. Accessory minerals are apatite, zircon and titanite, the latter in places forming coronas around oxides. The rock is inequigranular and far-reaching static recrystallisation is indicated by rather pervasive development of straight grain boundaries. The Stavsjö quarry also exposes meter long lenses of mafic high-pressure granulite, with a mineral assemblage dominated by brownish green hornblende, plagioclase, pink garnet, light green clinopyroxene and oxides. Hornblende, garnet and clinopyroxene occur in apparent textural equilibrium.

The Stavsjö gneiss is folded and has a strong axial-planar ductile foliation that dips ca 30° to the southeast. The folded gneissic foliation is cut by a number of seemingly undeformed sets of pegmatite

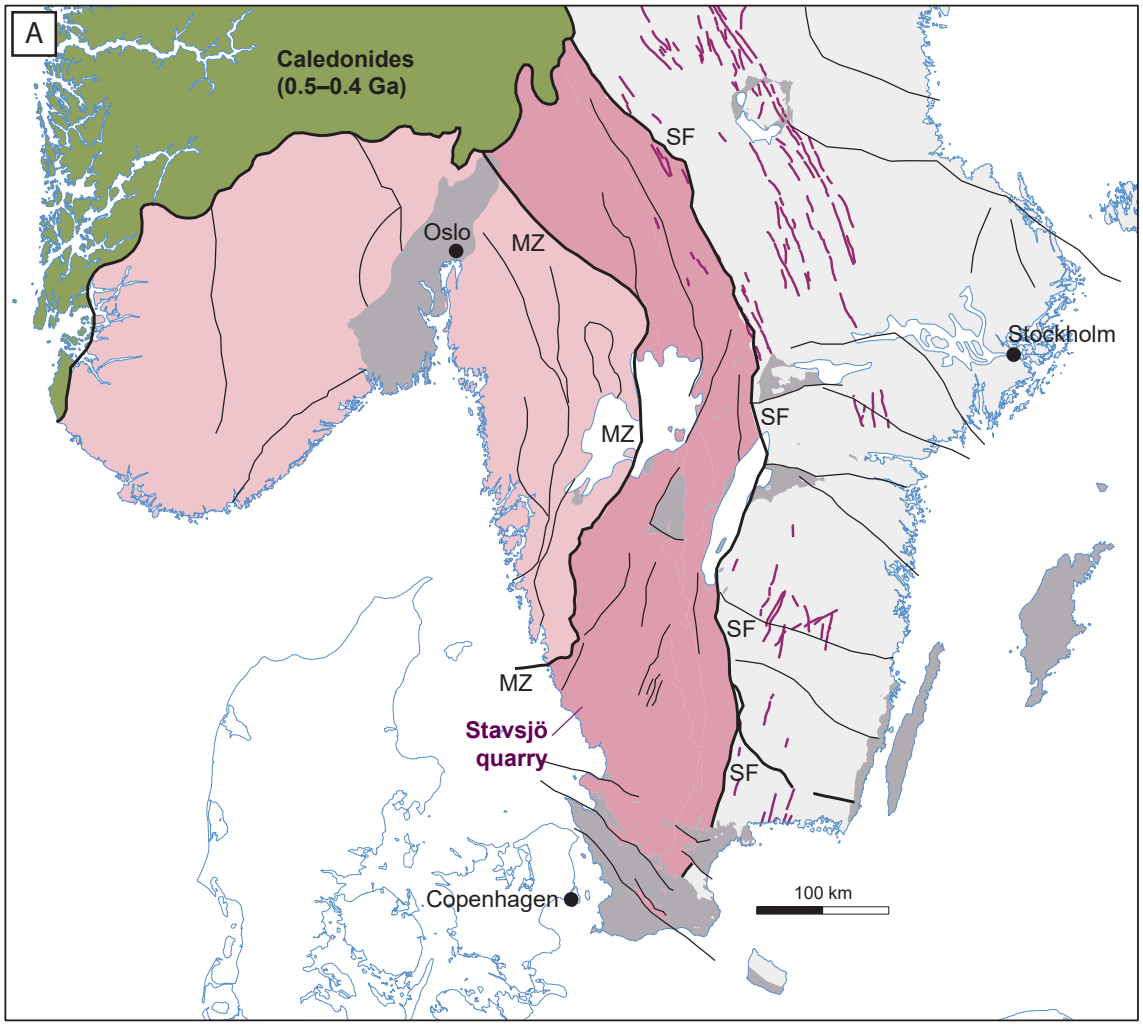

PHANEROZOIC ROCKS

Undifferentiated

SVECONORWEGIAN PROVINCE

Bedrock formed or deformed and metamorphosed during the 1.14–0.90 Ga Sveconorwegian orogeny

Western Sveconorwegian Province

Eastern Segment

MEZO- AND PALEOPROTEROZOIC PROVINCES

Bedrock unaffected by Sveconorwegian metamorphism and ductile deformation.

Bedrock formed or (and) deformed and metamorphosed during 1.92–1.66 Ga and 1.47–1.44 Ga orogenies

0.97–0.94 Ga dolerite (Blekinge-Dalarna Dolerites)

DEFORMATION ZONES

Major tectonic boundary

Conspicuous brittle and ductile deformation zones internal to the principal lithotectonic units

SF Sveconorwegian Front

MZ Mylonite Zone

Figure 1 A. Overview map showing major lithotectonic units and deformation zones in southern Sweden and southern Norway.

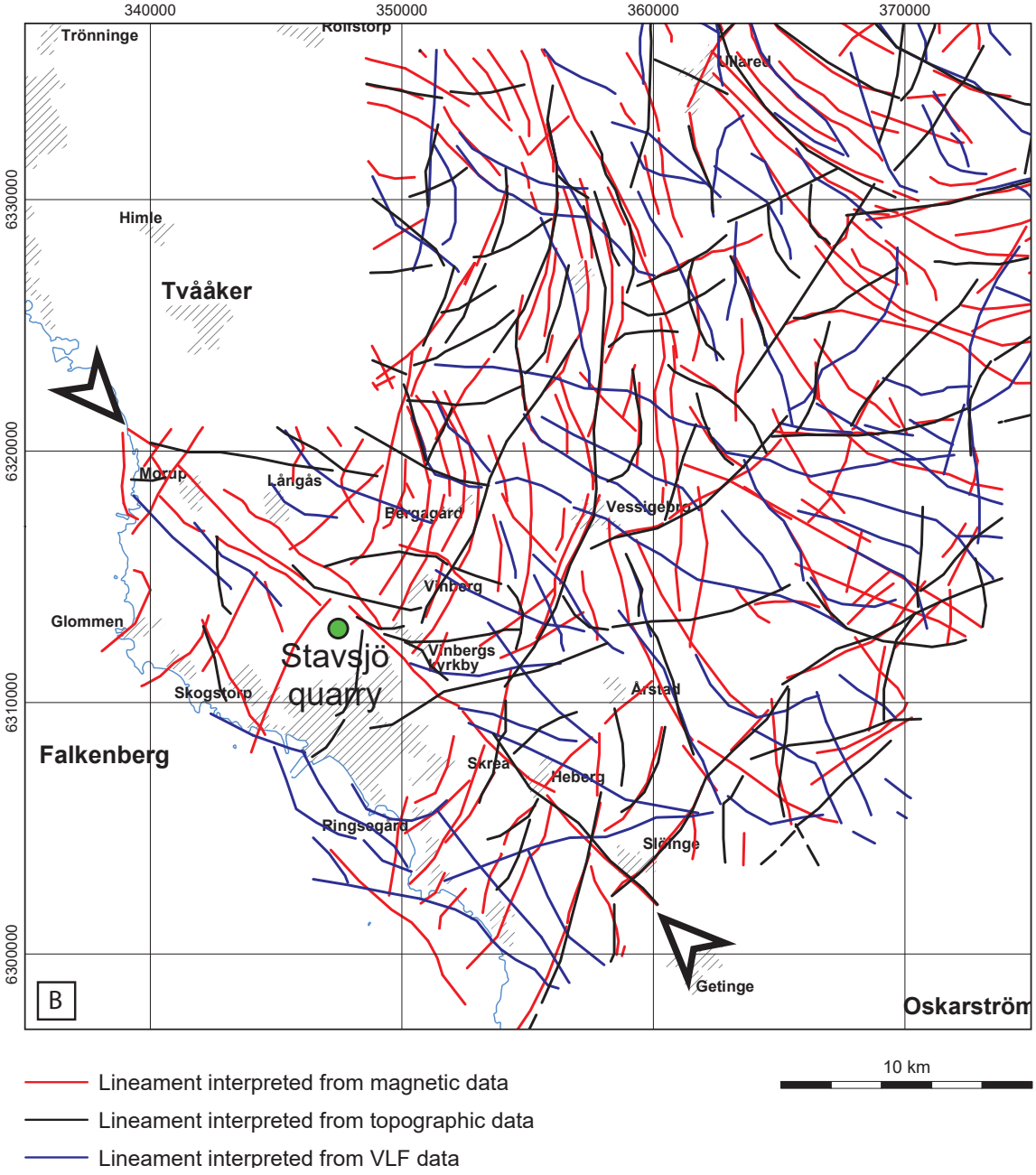

Figure 1 B. Map showing lineaments classified by the according geophysical background data used (VLF: Very Low Frequency). The arrows point out a dominant northwest–southeast striking magnetic lineament. More information on the interpretation of the lineaments is given by Andersson et al. (in press).

veins. Structurally late north-northeast trending subvertical dm-wide pegmatite dykes are also seen to cut the folded gneissic layering at a high angle.

Magnetic anomaly maps indicate two major sets of magnetic minima which are interpreted as brittle structures (Fig. 1B). One set trends northwest–southeast and the other set is oriented north to north-northeast–south to south-southwest. Lineaments interpreted from electromagnetic measurements (VLF) are predominantly oriented west-northwest–east-southeast. Topographic lineaments seem to follow both magnetic and VLF lineaments (Fig. 1B). One noticeable, dominant magnetic anomaly strikes northwest–southeast (marked by arrows in Fig. 1B). This orientation is parallel to the major Sorgenfrei-Tornquist Zone (Bergerat et al., 2007).

Methods

Twiss & Moores (2007, p. 38) suggest dividing fracture studies into four general categories:

(1) the distribution and geometry of the fracture system
(2) the surface features of the fractures (e.g., smooth, polished, slickensided)
(3) the relative timing of the formation of different fractures
(4) the geometric relationship of fractures to other structures.

In a first attempt to get control on these categories, surveys along three horizontal profile lines were undertaken along vertical walls in the quarry, and locations were marked wherever fractures crosscut the profile line. The profile lines trend 005°, 070°, and 100° and are named P005, P070, and P100 respectively (Fig. 2). For each fracture the orientation was recorded, as well as the spacing, and amount and direction of displacement. If the fractures were filled with minerals, the types of minerals were recorded, as well as the width and type of the infilling vein.

RESULTS

Overview

The general fracture pattern at the Stavsjö quarry can be observed along quarry walls that are oriented approximately north–south and east–west (Fig. 2). As can be seen in Fig. 3 all fractures crosscut the gently southeast dipping, pre-existing, ductile fabrics.

Figure 2. Aerial photograph of the Stavsjö quarry. The approximate positions of the mapped profiles P005, P100 and P070 are indicated by red lines. Orthophoto from Lantmäteriet.

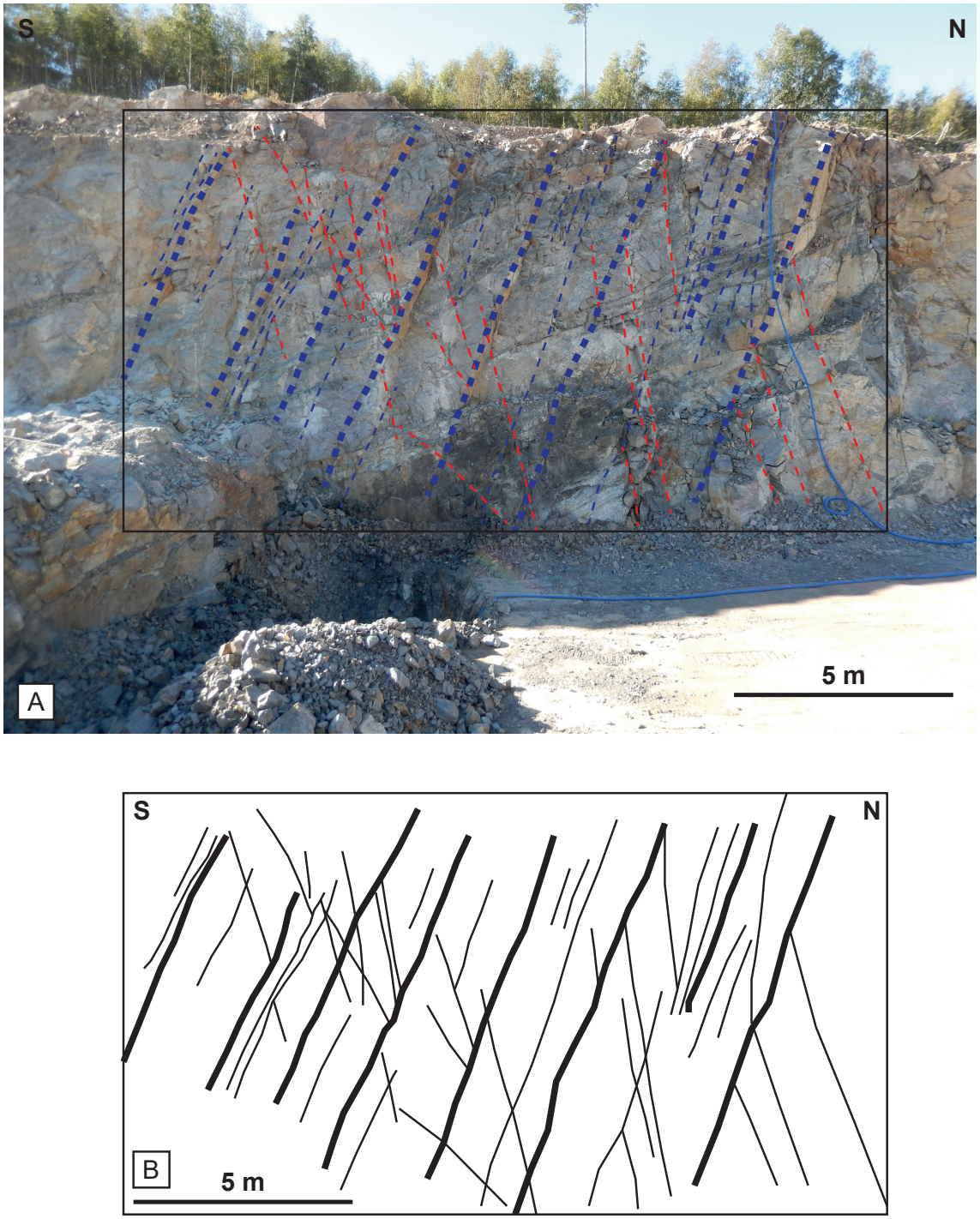

Figure 3 A. Photograph of the east-facing quarry wall. Traces of fractures are indicated. Blue: fractures dipping to the south-southwest. Red: fractures dipping to the north-northeast. The gently southeast dipping ductile fabric is visible from the lighter and darker colours originating from different mineralogical compositions. All fractures crosscut this ductile fabric. **B.** Fracture pattern extracted from the photograph. Thick lines emphasize dominant fractures.

Fracture orientation analysis

Along the three profiles, orientations of a total of 121 fractures were measured with a hand-held geological compass. An orientation analysis of all fractures indicates that there are at least two dominant sets of fractures with one set striking west-northwest–east-southeast and the other set

north-northeast–south-southwest (Fig. 4A, B). Dip angles for both sets of fractures peak at around 70°–80° (Fig. 4A). In a rose diagram, the strike data of these fractures peak at 110°–120° and 020°–030° respectively (Fig. 4C). When plotting the poles to the fracture planes in an equal area stereographic projection (Fig. 4D), it becomes obvious that the two main fracture sets each consist of pairs of conjugated fractures dipping towards opposite directions.

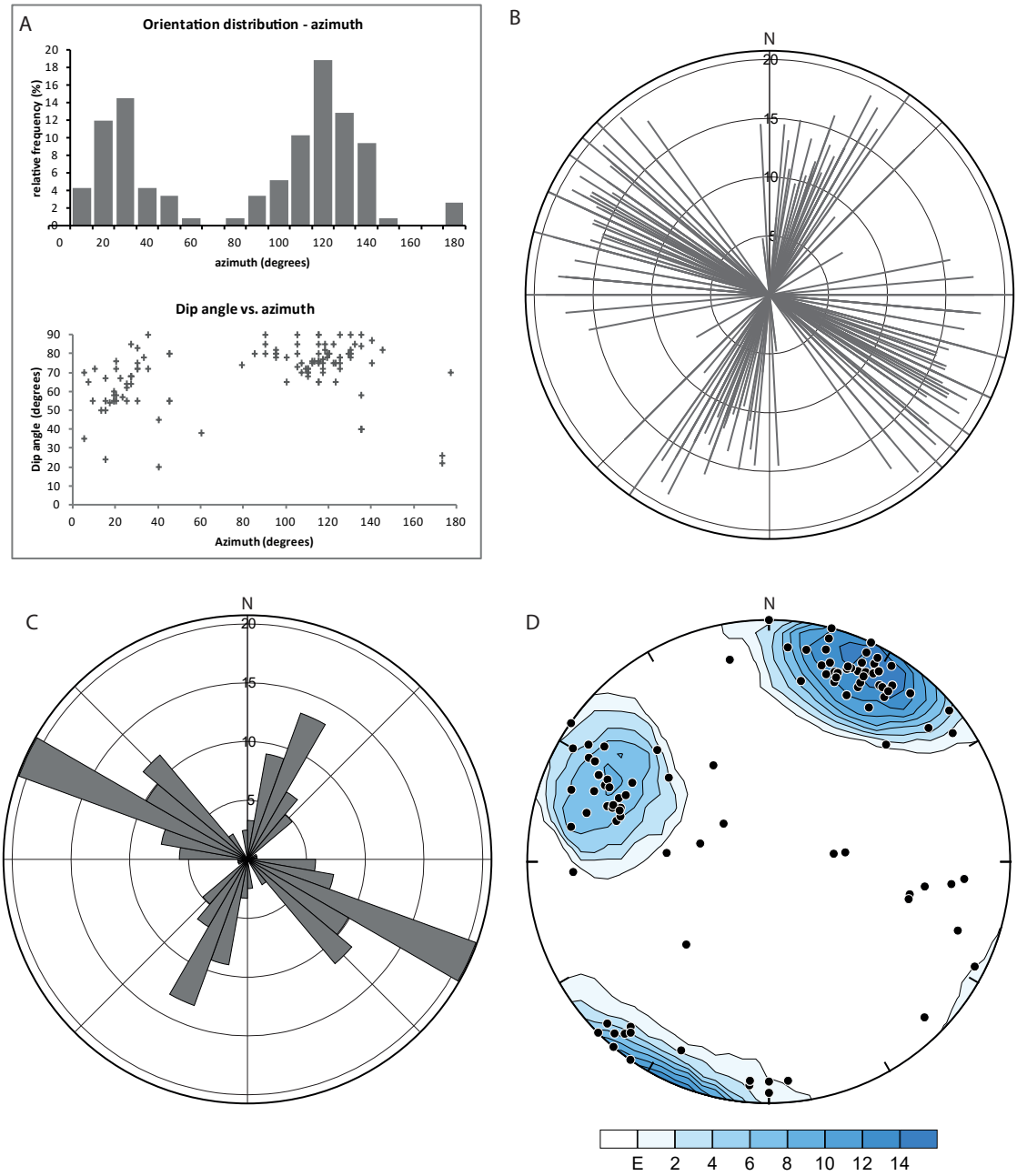

Figure 4. Orientation analysis of all fractures (N = 121). **A.** Histogram with 10°categories, showing relative frequency of measured fracture azimuths (top). Diagram showing distribution of fracture dip angles vs. fracture azimuths (bottom). **B.** Azimuth raw data plotted in a rose diagram. The length of the lines varies with the dip angle. The circles represent total frequency. **C.** Rose diagram of fracture azimuth data with 10°categories. The circles represent total frequency. **D.** Poles to fracture planes plotted on a lower hemisphere equal area stereographic projection. Density distribution contours using method by Kamb (1959). (E = 3 x standard deviation, contours are multiples of standard deviation above E).

Spatial distribution of fractures within strike categories

The spacing between fractures was measured along the respective profiles. Since the profiles lay roughly perpendicular to the dominating fracture azimuths, the spacing was not corrected for potential deviation of the fracture azimuths from normality to the profile line. In addition, no correction was made for different dip angles. The mean spacing and standard deviations for the fractures are calculated for different strike categories and presented in table 1.

The spacing analysis shows that the fractures within the 0–45 and 90–135 strike categories have an average spacing of ca. 0.5 m. This means that along a 100 m long profile across strike it can be expected to encounter ca. 200 fractures of that strike category. Considering the low number of fractures observed in the 180–225 and 270–315 strike categories and their large standard deviations it is difficult to interpret the calculated average spacing. It is not clear whether this low number is indeed a natural effect or whether it results from biased measurements.

Types of observed fractures

Only natural fractures were taken into account. Fractures induced by blasting are easily recognised as irregular fracture zones around the drill holes, and they were excluded from the measurements.

Fractures without displacement and without infilling vein

Open fractures without mesoscopically observable displacement and without infilling veins are the most common type of fractures. These fractures have apertures on the mm scale or less. Sometimes, a thin coating of very fine-grained material can be observed on the fracture surfaces. The mineralogy of the fine-grained material could not be determined in the field.

Fractures with displacement

Very rarely, geological markers such as pegmatites or other fractures are noticeably offset across the fractures rendering those fractures true faults or at least shear fractures. The displacements are in the mm and rarely dm scale (Fig. 5). In all observed cases, the displacement was down-dip, which is locally also indicated by slickenlines on the fracture surface.

Along profile P100, it was possible to follow a subhorizontal pegmatite for 12.75 m and measure displacements of the pegmatite marker across the observed faults. When plotting the displacement values against the strike of the fractures, it shows that normal faulting occurs predominantly along west-northwest dipping fractures (Fig. 6). These shear fractures also accommodate larger displacements than the conjugated, east-southeast dipping fractures (Fig. 6).

Locally, also the conjugated east-southeast dipping fractures are displaced along the west-northwest dipping shear faults, indicating that the observed normal faulting may be due to a later reactivation of the west-northwest dipping fractures. A cm-wide discoloured alteration halo can be observed along these reactivated fractures (Fig. 5) which seems to be missing along the east-southeast dipping fractures.

Table 1. Spacing analysis for fractures according to strike categories.

Strike category (°)	Mean spacing (m)	Standard deviation (m)	Number of fractures
0–45	0.53	0.64	34
180–225	2.1	1.5	7
90–135	0.52	0.57	47
270–315	1.01	2.1	11

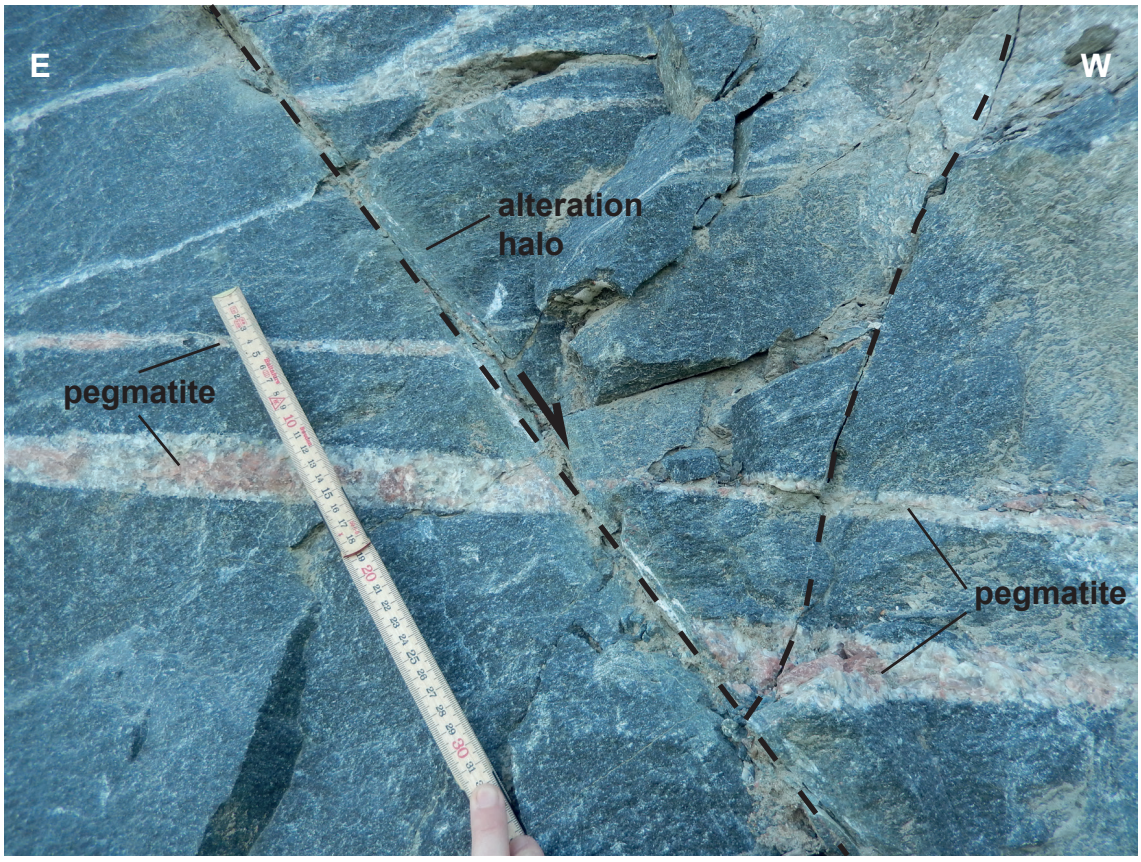

Figure 5. Down-dip normal faulting of pegmatite veins along a west-northwest dipping shear fracture at profile P100. No displacement of the pegmatite occurred across the subordinate, east-southeast dipping conjugate fracture. Instead, this fracture itself is displaced along the west-northwest dipping shear fracture. The angle between the two fractures is ca. 60°. The fact that displacement only occurred on one fault may indicate a later reactivation of that fault. Note also the light grey to green alteration halo around the west-northwest dipping fracture.

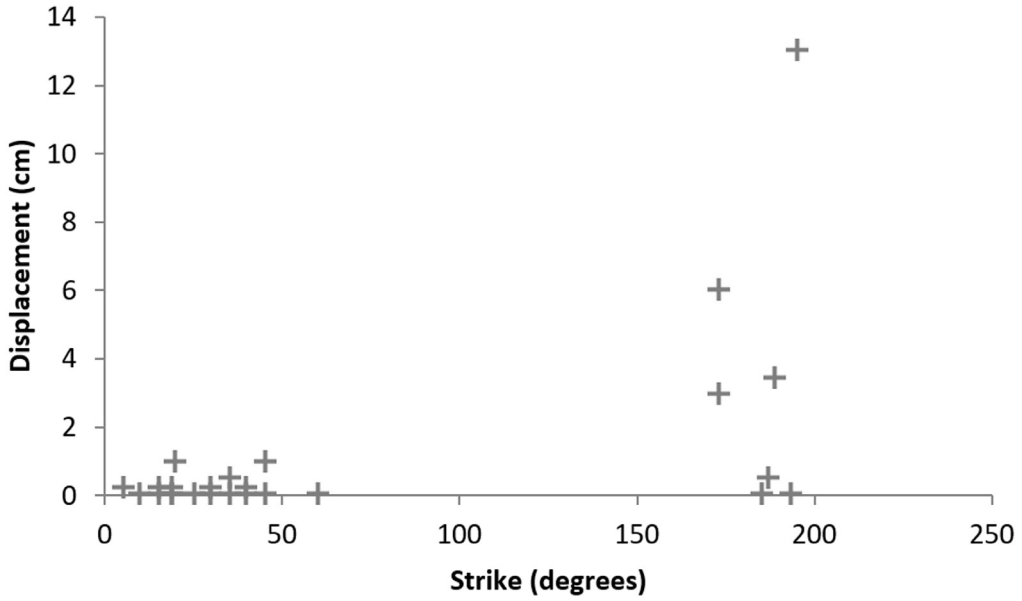

Figure 6. Diagram showing relationship between the strike of a fracture and the amount of displacement of a horizontal pegmatite vein along profile P100. West-northwest dipping fractures are fewer but seem to take up the bulk of the normal fault movement.

Fractures with infilling veins and breccia veins

Fractures with infilling veins were predominantly observed along profile P005. Here, the majority of the south-southwest dipping fractures have got a calcite filling that can be up to several centimetres thick. The north-northeast dipping fractures contain only thin coatings of calcite or are not infilled (Figs. 7 and 8).

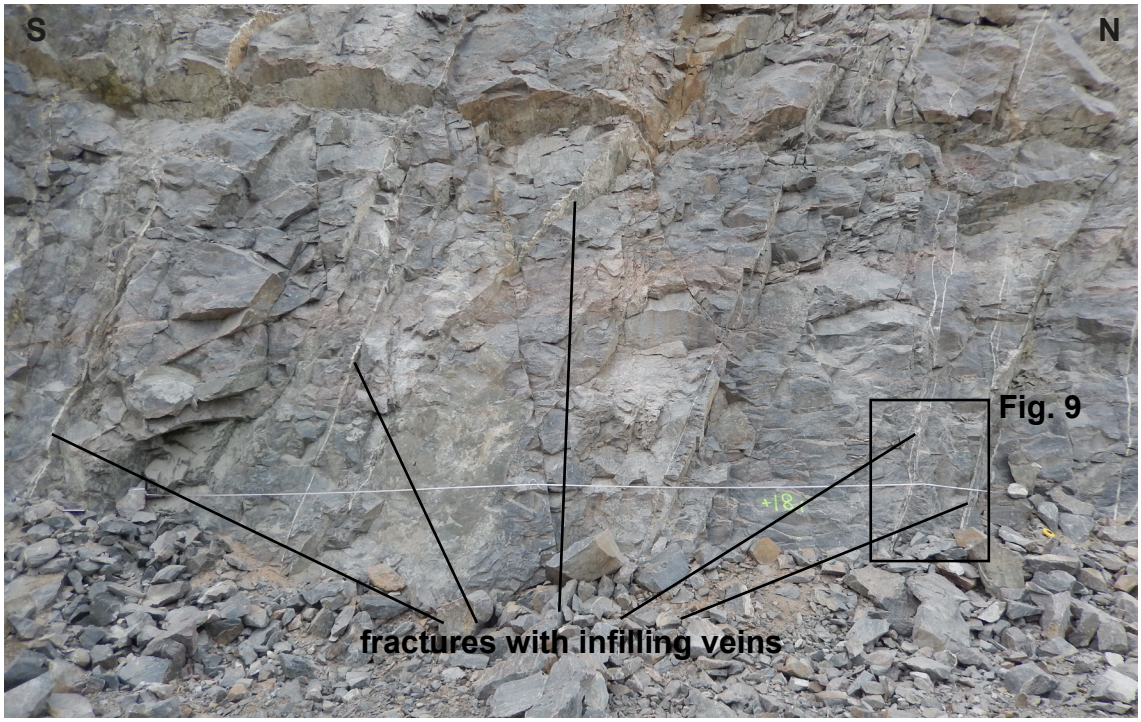

Figure 7. Fractures along profile P005, east-facing wall. Note that predominantly the south-southeast dipping fractures have large apertures and are filled with white calcite veins. The tape is extended to 10 m. The box indicates the position of the photograph in Fig. 9.

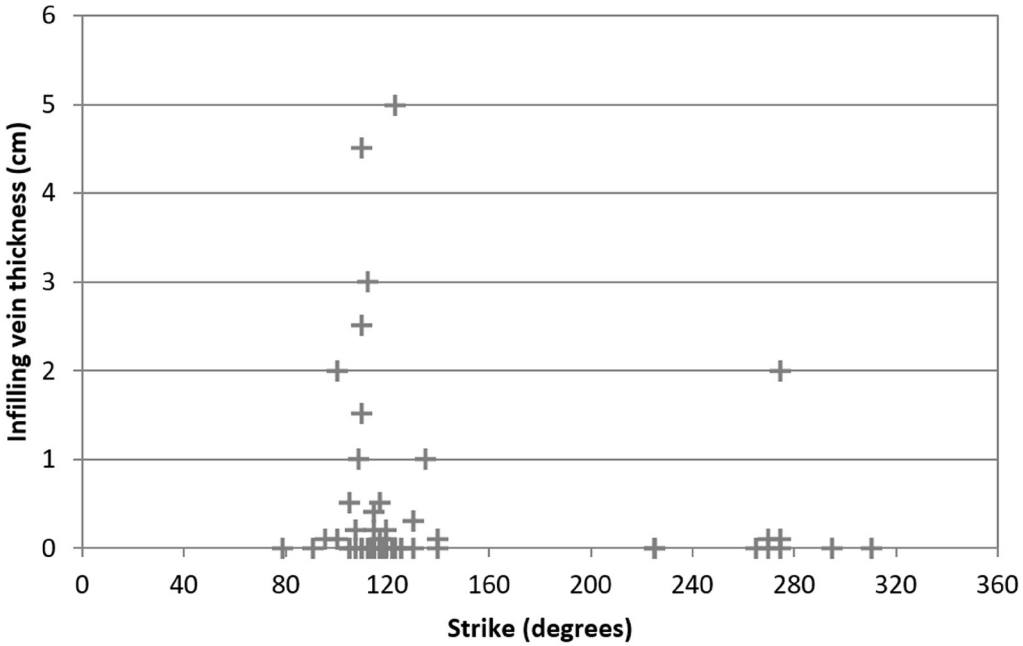

Figure 8. Diagram showing infilling calcite vein thickness versus strike of the fractures along profile P005. The fractures striking around 110–120° seem to be filled more frequently by veins than their conjugate counterparts.

Some of the observed fracture infilling veins are not easily interpreted. Generally, they seem to reactivate an older fracture system, but also create new fractures subparallel to the older fracture system (Fig. 9). They branch (Fig. 10), and form vein networks and breccia veins that contain wall rock fragments.

Very rarely, fractures contain other fracture minerals such as epidote, chlorite and a red mineral that could not be identified in the field.

Figure 9. Details of a calcite vein brecciating the wall rock. The part of the vein lying below the tape measure is 4.5 cm broad and has got a striped pattern, which may indicate reactivation of a presumably older fracture by a crack-seal mechanism. The parts of the breccia vein lying above the tape measure seem to partially infill a north-northeast dipping fracture, where this one intersects with the south-southwest dipping one. Further up, a new vein network is formed subparallel to the older south-southwest dipping fractures.

Figure 10. Branching, fracture-infilling calcite vein dipping towards the south-southwest.

INTERPRETATION AND DISCUSSION

The high degree of symmetry of the two conjugated fracture pairs indicates that the fractures originally formed an orthorhombic fracture pattern (e.g. Fossen, 2010, p. 193) in a stress regime where the maximum principal stress σ_1 was subvertical and where the intermediate and minimum principal stresses $\sigma 2$ and $\sigma 3$ were subhorizontal. The reactivation of some of the west-northwest dipping fractures as normal faults probably also happened during these stress conditions indicating that $\sigma 3$ was oriented west-northwest–east-southeast.

It is questionable when the south-southwest dipping, calcite-filled fractures formed, but several observations suggest that they formed in a stress regime that differed from the previous one; no shear displacement was observed along these fractures, and predominantly fractures dipping to the south-southwest were used as fluid pathways indicating that $\sigma 3$ was oriented south-southwest–north-northeast but may not have been entirely horizontal. New fracture networks were formed which may point to a hydraulic fracturing event. The branching of the calcite veins and formation of breccia veins, indicates high strain rates and high differential stresses at the fracture tips. Such a situation can be achieved when the fluid pressure exceeds the overburden pressure.

On a regional scale, the orientation of the fractures that strike west-northwest–east-southeast suggests that they are related to the major northwest–southeast trending magnetic lineament pointed out in Fig. 1. The calcite filled fractures may actually correspond to the west-northwest–east-southeast oriented electromagnetic (VLF) anomalies and may represent potentially water-bearing structures, subordinate to the major northwest–southeast striking magnetic anomaly.

The north-northeast–south-southwest striking fractures match well with the somewhat shorter, northeast–southwest trending magnetic lineaments presented in Fig. 1. North-northeast–south-southwest striking fractures and faults are common in bedrock exposures in the surrounding gneiss complex (Andersson et al. in press) as well as on a regional scale in the Eastern Segment south of Lake Vänern (Andreasson och Rodhe 1992, Wik et al. 2006). These fractures and brittle faults have also been coupled to the development of the Vättern graben fault system (cf. Andreasson och Rodhe 1992). The occurrence of north-northeast–south-southwest striking 0.97–0.94 Ga old dolerites in the Eastern Segment and the foreland region east thereof (the Blekinge Dalarna Dolerites, Söderlund et al., 2005) suggests that a crustal scale extensional stress field was already established in late Sveconorwegain time. This is supported by the occurrence of late-Sveconorwegian low-grade metamorphic alterations (epidotization) along north-northeast– south-southwest trending fractures, documented in several quarries in the internal parts of the Eastern Segment, including the Stavsjö quarry (La Roche et al. 2014). Jakobsson et al. (2014) suggest that reactivation of the north-northeast striking faults and fractures may have continued even into the late Holocene.

In order to deduce a potential connection between the observed brittle structures at Stavsjö quarry and major tectonic structures including the northwest–southeast trending Sorgenfrei-Tornquist Zone to the southwest, further studies of brittle structures in surrounding quarries are necessary.

It needs to be pointed out that gently dipping fractures are underrepresented in the data collected for this pilot study. This is because these fractures simply do not intersect with the horizontal profiles. In order to record the gently dipping fractures, it would be necessary to map along vertical profiles which was, however, not feasible during this study and is a general problem for fracture mapping in quarries. It is therefore recommended to use other techniques such as photogrammetry to map fracture systems in 3 dimensions.

CONCLUSIONS

Simple profile-mapping along vertical quarry walls has resulted in the interpretation of two sets of brittle fractures. At least two reactivation phases, under different stress conditions, are deduced from the observations.

Overall, the orientations of the fractures measured at Stavsjö quarry match the orientations of regional geophysical lineaments, indicating that these lineaments do indeed represent brittle structures. This limited field study suggests that the brittle structural pattern is scale-independent.

REFERENCES

Andreasson P.-G., & Rodhe, A., 1992: The Protogine zone. Geology and mobility during the last 1.5 Ga. Swedish Nuclear Fuel and Waste Management Co, TR 92-21.

Bergerat, F., Angelier, J., & Andreasson, P. G., 2007: Evolution of paleostress fields and brittle deformation of the Tornquist Zone in Scania (Sweden) during Permo-Mesozoic and Cenozoic times. *Tectonophysics, 444(1),* 93–110.

Fossen, H., 2010. Structural geology. Cambridge University Press, 463 p.

Jakobsson, M., Björck, S., O'Regan, M., Flodén, T., Greenwood, S.L., Swärd, H., Lif, A., Ampel, L., Koyi, H., & Skelton, A., 2014: Major earthquake at the Pleistocene-Holocene transition in Lake Vättern, southern Sweden. *Geology 42(5),* 379–382.

Kamb, W.B., 1959: Ice petrofabric observations from Blue Glacier, Washington, in relation to theory and experiment. *Journal of Geophysical Research 64,* p. 1891–1909.

La Roche, A., Stark, M., Johansson, L., Rhede, D., & Hansen, E.C., & Bornhorst, T.J., 2014: Hydrothermal formation of epidote in felsic compositions: examples from Sweden and northern Michigan. Geological Society of America annual meeting in Vancouver, British Columbia, Canada. Abstract volume.

Lundgren, L. 2012. Variation in rock quality between metamorphic domains in the lower levels of the Eastern Segment, Sveconorwegian Province. Unpublished MSc thesis, Lund university. 64 p.

Twiss, R.J., Moores, E.M. 2007. Structural Geology. W.H. Freeman and Company, 736 p.

Wik, N.-G., Andersson, J., Bergström, U., Claeson, C., Juhujuntti, N., Kero, L., Lundqvist, L., Möller, C., Sukotjo, S. & Wikman, H., 2006: Beskrivning till regional berggrundskartan över Jönköpings län. *Sveriges geologiska undersökning K 61,* 60 s.